



Chilles, J., Croxford, A., & Bond, I. (2015). Design, application and validation of embedded ultrasonic sensors within composite materials. In P. Shull (Ed.), *Structural Health Monitoring and Inspection of Advanced Materials, Aerospace, and Civil Infrastructure 2015* (Vol. 9437). (Proceedings of SPIE). <https://doi.org/10.1117/12.2083944>

Peer reviewed version

Link to published version (if available):
[10.1117/12.2083944](https://doi.org/10.1117/12.2083944)

[Link to publication record in Explore Bristol Research](#)
PDF-document

Copyright 2015 Society of Photo-Optical Instrumentation Engineers. One print or electronic copy may be made for personal use only. Systematic reproduction and distribution, duplication of any material in this paper for a fee or for commercial purposes, or modification of the content of the paper are prohibited.

University of Bristol - Explore Bristol Research

General rights

This document is made available in accordance with publisher policies. Please cite only the published version using the reference above. Full terms of use are available:
<http://www.bristol.ac.uk/red/research-policy/pure/user-guides/ebr-terms/>

Design, application and validation of embedded ultrasonic sensors within composite materials

James Chilles*, Anthony Croxford, Ian P Bond

Advanced Composites Centre for Innovation and Science, University of Bristol, Queen's Building, Bristol BS8 1TR, UK

ABSTRACT

The layer wise construction of laminated composites offers the potential to embed sensors within composite structures. One possible solution is the embedding of sensors that are inductively coupled to an external probe; which allows for the efficient contactless transfer of electrical signals to the sensor. Embedding sensors within structures is an attractive option, due to the physical protection offered to the sensor by the host structure. However, for embedding sensors to be viable, sensor integration must result in minimal degradation of the laminates mechanical performance. This work focuses on designing embedded inductively coupled sensors for structural performance. A suitable sensor coating for the sensor unit was identified using interlaminar shear strength testing. Sensors were then embedded into quasi-isotropic four-point bend flexural strength specimens, and different embedding strategies demonstrated. In addition to providing the sensor with physical protection, embedding sensors within a composite host offers the additional benefit of monitoring the curing process of the surrounding composite. A single inductively coupled sensor was embedded into a large glass fiber epoxy plate, and the measured guided wave pulse echo response used to monitor the curing process. This novel cure monitoring technique was then benchmarked against direct scanning calorimetry.

Keywords: Embedded, Inductively coupled, Structural integrity, Composites, Ultrasonic, Cure monitoring

1. INTRODUCTION

Fiber reinforced composites possess high specific stiffness and strength, which has led to their application in weight critical aerospace structural components. However, composite materials are susceptible to impact damage. Even relatively low energy impacts can result in a complex network of delaminations and matrix cracks, which are difficult to detect by visual inspection¹. Current non-destructive evaluation processes for aerospace structures such as C-Scan and X-Ray can lead to significant downtime, incurring high costs. This research is concerned with the development of a network of sensors embedded within composite materials. Such a system could increase the automation of inspection, reducing its difficulty, potentially leading to reduced downtime and costs for inspection programs.

The specific sensing system investigated in this work is an inductively coupled transducer system (ICTS) as described in the work of Zhong et al^{2,3}. The ICTS is a three coil network (Figure 1a). The sensor unit embedded within the composite is comprised of an inductance coil (termed the transducer coil, Figure 1a) connected to a piezoelectric transducer. The embedded unit is passive and has no power generation or storage capability, only becoming active once excited by an inspection wand. The wand contains two additional coils (termed the transmitter and receiver coils, Figure 1a). The transmitting coil is connected to the output, and the receiving coil connected to the input of the ultrasonic processing equipment. The inductive coupling between the three coils allows for electrical signals to be wirelessly transferred between the embedded sensor and ultrasonic instrumentation. The removal of the requirement to store and generate power, enables the size of the sensor to be minimized; reducing both the structural weight and disruption caused to the surrounding composite structure, when compared with embedding larger sensors.

Embedding sensors within structures is an attractive option, as the embedded unit is provided with physical protection by the host structure, however for embedment to be feasible the sensors must be integrated without significantly reducing the mechanical performance of the host. In this paper the effect of embedding slim inductively coupled sensors (Figure 1b and Table 1) is evaluated and embedding strategies demonstrated. A suitable coating material to encapsulate the inductively coupled sensor was identified using interlaminar shear strength testing. The encapsulating layer provides two functions; electrical insulation from the conductive carbon fibers commonly used to construct aerospace structures, and a strong mechanical bond with the polymer matrix of the surrounding composite. The influence of embedding technique,

sensor geometry and through-thickness embedding location were evaluated using four-point bend flexural strength testing. To characterize the sensors under the critical compressive load case ⁴, sensors were embedded towards the compressive surface of the flexural specimens (discussed in more detail in section 2.2.1).

In addition to monitoring the structure for damage, embedding sensors within composite materials provides the additional benefit of monitoring the manufacturing process of the host structure. The most commonly used manufacturing route for structural aerospace components are autoclave processes ⁵; in which sheets of B-staged resin pre-impregnated with reinforcing fibers (prepreg) are laid onto tooling with the desired geometry, and cured inside a chamber (termed an autoclave) held at elevated temperature and pressure. When curing composite structures on an industrial scale the aim is to fully cure the structure in the minimum amount of time ⁶. Real time cure data provided by the ICTS could allow identification of exactly when the composite is fully cured; improving both quality control and production economy. Various researchers ^{7,8,9} have monitored the cure of polymers using ultrasonic techniques. The majority use transducers embedded in the tooling to make bulk wave measurements across the thickness of curing specimens ^{7,8}. The significant physical changes occurring during the cure process are related to the ultrasonic parameters associated with the propagating waves, and cure progress identified. Embedded sensors have been used to monitor the curing process, Lin and Chang ¹⁰ monitored the cure of composite materials using an embedded smart layer, by measuring the variation in pitch catch measurements between adjacent sensing nodes. This study presents a novel cure monitoring technique, were a single inductively coupled sensor (Figure 1b) monitors the cure cycle of a large glass fiber epoxy plate. The sensor was embedded into the laminates stacking sequence during layup, and wireless measurements recorded throughout the curing process. The performance of this technique was benchmarked against direct scanning calorimetry (DSC), an established technique for monitoring the cure of polymers ^{9,11,12}.

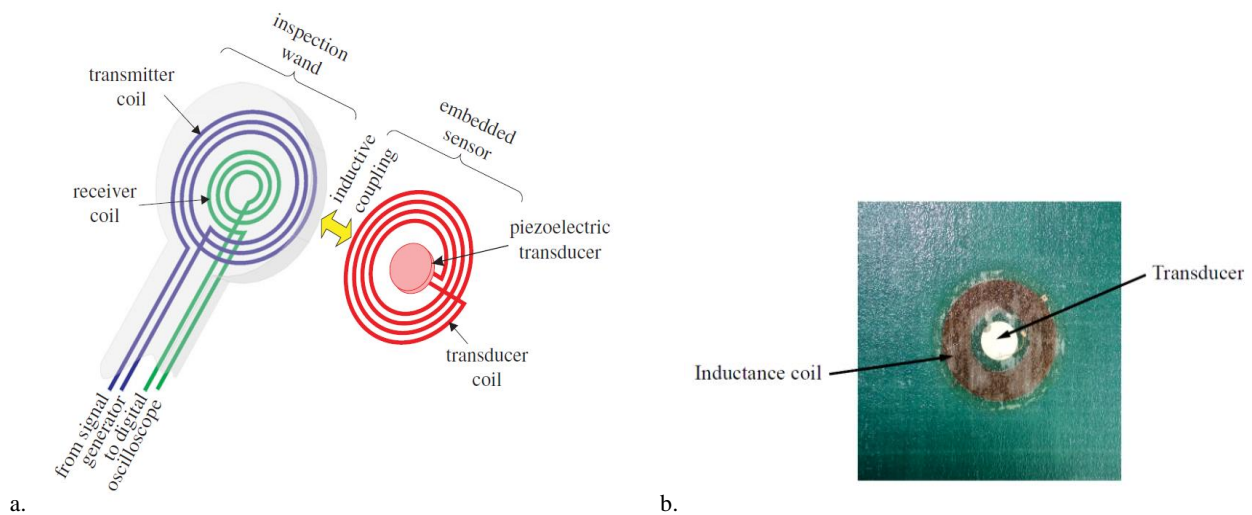


Figure 1a. Three coil system, displaying the inductive coupling between the transmitter, embedded and receiver coils.³ b. Sensor embedded into a glass fiber epoxy plate.

Table 1. Dimensions of the components within the sensor unit shown in Figure 1b.

Component	Piezoelectric disk transducer	Inductance coil
Outer Diameter (mm)	10	50
Thickness (mm)	0.3	0.12

2. SENSOR DESIGN AND EMBEDDING

The sizing of the inductance coil and selection of piezoelectric transducer for optimal ultrasonic performance was carried out in a previous study³. The choices made in this work were primarily concerned with designing the inductively coupled sensors for structural performance.

2.1 Interlaminar shear strength testing

For the sensors to be embedded inside carbon fiber reinforced polymers (material system commonly used to construct structural aerospace components¹) each sensor must be encapsulated within an electrical insulator. Interlaminar shear strength testing was used to assess the ability of different electrical insulators (Table 2) to form a strong mechanical bond with a composite material.

2.1.1 Specimen manufacture

The interlaminar shear specimens were manufactured from a unidirectional glass fiber epoxy prepreg material system (Hexcel, E-Glass 913), each specimen was unidirectional with a layup of $[0^\circ]_{14}$. The stacking sequence was assembled using the hand layup process, and each potential sensor coating (Table 2) was embedded at the midplane. The assembled laminates were cured inside an autoclave at a temperature of 125°C and pressure of 7 bar for 1 hour. Once cured, the specimens were cut to a length of 20 mm and width of 10 mm, using a water cooled diamond saw.

Table 2. Interlaminar shear specimens.

Experimental group	Encapsulating Layer	Surface treatment	Sample size	Total thickness (mm)
Control	N/A	N/A	5	2.06 ± 0.09
A	Bond ply	Acrylic adhesive	5	2.14 ± 0.07
B	Kapton	Diethylenetriamine	5	2.26 ± 0.07
C	Upilex	Diethylenetriamine	5	2.19 ± 0.06

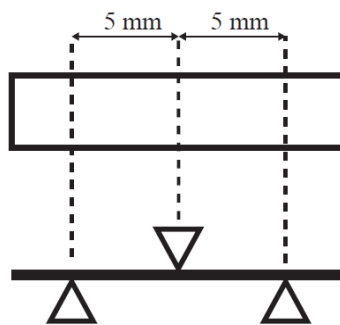


Figure 2. Three-point bend interlaminar shear testing geometry.

2.1.2 Experimental method

The interlaminar shear strength testing was carried out in accordance with BS EN 2563:1997. The specimens were loaded in a three-point bend configuration (Figure 2). The testing was carried out with a loading rate of 1 mm/min. The four experimental groups are summarized in Table 2.

2.1.3 Results

The results of the interlaminar shear strength testing are shown in Figure 3. The two films in experimental groups B and C (Table 2), produced a reduction in the interlaminar shear strength of the beams. In each case a delamination was seen to propagate along the interface between the embedded layer and the composite. No failure was seen to occur between the interface of the embedded bond ply layer and composite (Group A, Table 2), failure of the specimens occurred between the plies of the composite, with the interface between the embedded layer remaining intact. Of the three potential sensor coatings the bond ply (Group A, Table 2) provided the best performance, and was selected as the layer to encapsulate the sensors in the subsequent flexural strength testing.

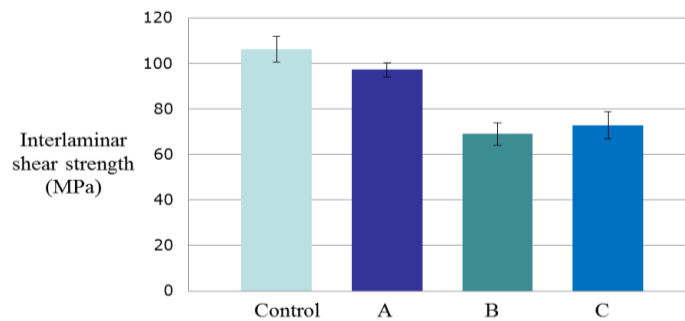


Figure 3. Interlaminar shear strength results

2.2 Four-point bend flexural strength testing

Four-point bend flexural strength testing was used to evaluate two different embedding strategies (Figure 4a and b). The sensors were embedded inside a quasi-isotropic laminate, widely used in industrial applications (Figure 5). The comparison between the laminates containing sensors and the control specimens, allowed the effect of sensor integration to be evaluated.

2.2.1 Specimen manufacture

The flexural strength specimens were manufactured from a unidirectional glass fiber epoxy prepreg (Hexcel, E-Glass 913). The stacking sequence of each laminate was assembled using the hand layup process. The manufacturing method of each laminate varied depending on the chosen method of sensor embedment. Sensors embedded using the forming technique (Figure 4a and Group E, Table 3) were placed into the laminates stacking sequence, and subsequent plies laid. The forming method maintains continuous plies, but introduces fiber waviness into the plies above the sensor (Figure 4a). Figure 4b shows a sensor embedded using the cut ply technique, three plies of prepreg were cut and a region equal to the total length of the sensor unit removed. Prior to embedding the sensor was molded into a rectangular profile, with epoxy resin film (Hexcel, 913 resin film) laid onto the coil to compensate for the difference in thickness between the transducer and coil. The cut ply method (Figure 4b) minimizes the induced fiber waviness, but does not maintain continuous fibers. All of the laminates were cured at 125°C for one hour with 7 bar of pressure, the cycle contained a 30 minute dwell at 95°C. Specimens were cut to a length of 160 mm and width of 20 mm, using a water cooled diamond saw. The laminate layup (a quasi-isotropic widely used in industrial applications), and through-thickness embedding locations for experimental groups D and E (Table 3) are shown in Figure 5.

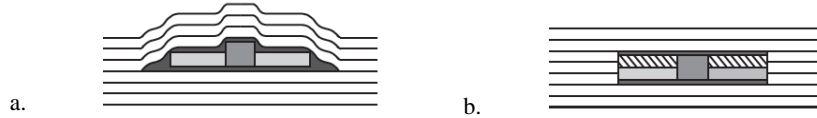


Figure 4a. Sensor embedded using the forming method. b. Sensor embedded using the cut ply technique.

Table 3. Flexural strength specimens

Experimental Group	Embedding method	Sample size	Total thickness (mm)
Control	N/A	5	4.96 ± 0.04
D	Cut ply	5	4.89 ± 0.14
E	Formed	5	5.37 ± 0.17

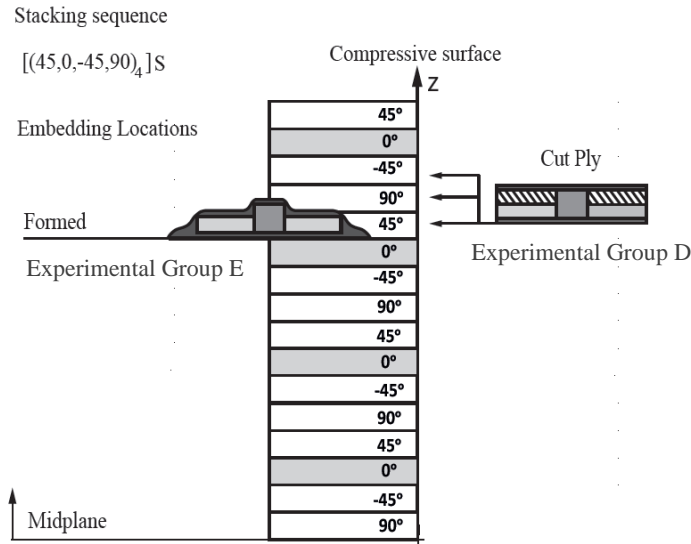


Figure 5. Laminate layup and embedding locations for the specimens in Table 3.

2.2.2 Experimental method

Four-point bend flexural strength testing according to ASTM D6272 10 was chosen to characterize the behavior of flexural specimens with sensors embedded towards the compressive surface (Figure 5). The experimental test setup is shown in Figure 6. The testing was carried out with a support to load span ratio of 2:1, and a support span to thickness ratio of 28:1. A loading rate of 5 mm/min was applied to all of the specimens. The experimental groups are displayed in Table 3. The embedding methods are shown in Figures 4a and b, and the embedding locations of the tested embedding methods are shown in Figure 5.

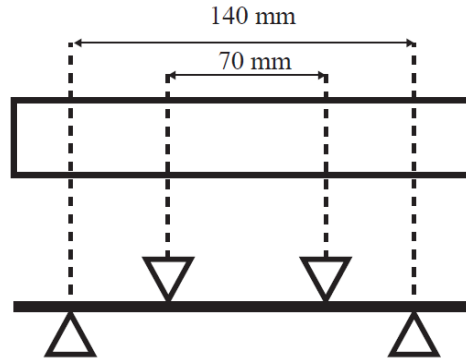


Figure 6. Three-point bend interlaminar shear testing geometry.

2.2.3 Results

The four-point bend flexural strength results are shown in Table 4. All of the tested specimens failed in a tensile failure mode. The gradual growth of delaminations led to the breaking of fibers on the underside of the flexural specimens (Figure 7), indicating that embedding of the sensors in specimen groups D and E did not significantly reduce the host laminates compressive strength. The presence of the cut ply sensor embedded in specimen group D had no effect on the flexural strength of the beams; each specimen behaved in the same way as the control group. This result shows that cut ply sensors can be successfully integrated within composite structures providing the load bearing plies are not cut. The observed flexural strength of experimental group E is lower than that of the control group (Table 4), however this is not due to the presence of the sensor reducing the strength of the beams. The localized increase in sensor thickness at the center of the specimens caused by sensor integration (Table 3), affected the flexural strength calculations. The tensile failure mode of experimental group E (Table 4) indicates that the presence of the formed sensor (embedded towards the compressive surface) did not initiate premature failure of the flexural specimens. The tensile failure shows that by ensuring the fiber waviness induced in load bearing plies is minimized, formed sensors can be embedded without reducing the mechanical performance of the host structure. In no case was a delamination seen to propagate from either of the embedded sensor configurations; which supports the selection of bond ply as an encapsulating layer for the inductively coupled sensors.

Table 4. Flexural strength results.

Experimental group	Embedding technique	Flexural Strength (MPa)	Failure Mode
Control	N/A	698 ± 29	Tensile Failure
D	Cut ply	699 ± 31	Tensile Failure
E	Formed	671 ± 32	Tensile Failure

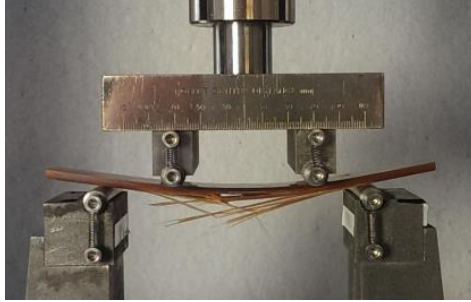


Figure 7. Tensile failure mode of the flexural specimens.

3. CURE MONITORING

Having shown that sensors can be embedded with minimal impact on structural performance, the unique benefits offered by embedding sensors within composite materials were explored. Embedding the sensors within a composite structure not only offers physical protection from the operating environment, but provides a means monitoring the curing process of the host structure. The cure monitoring ability of the ICTS was demonstrated by monitoring the cure of a large glass fiber epoxy plate, in an autoclave type manufacturing process. The ability of the ICTS to monitor the cure of composite prepreg material was then benchmarked against DSC (an established cure monitoring technique) ^{9,11,12}.

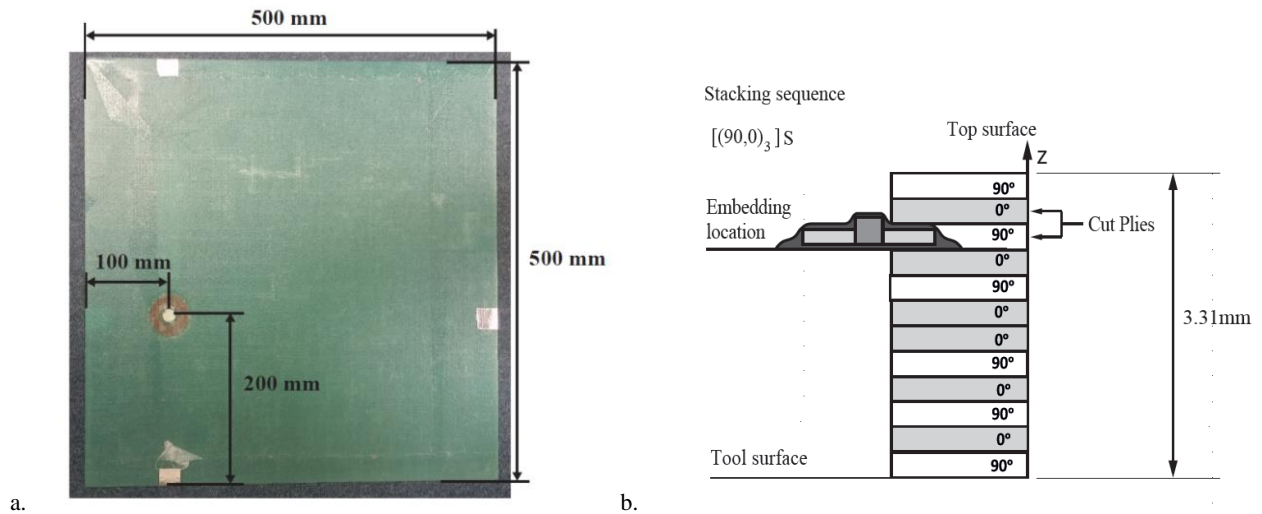


Figure 8a. Dimensions and sensor location of the cured composite plate. b. Stacking sequence and through-thickness embedding location of the sensor unit.

3.1 Manufacture.

The cure of a glass fiber epoxy prepreg system (Gurit, Glass fiber reinforced SE70) was monitored during this study. The dimensions of the plate are shown in Figure 8a, and the embedding location and laminate layup in Figure 8b. The sheets of unidirectional prepreg were laid down onto an aluminum tool plate by hand, with the fiber orientations shown in Figure 8b. A 50 mm diameter region of prepreg was cut from the plies shown in Figure 8b, and the sensor unit placed into the removed region of prepreg. The laminates stacking sequence was completed, and the assembled laminate sealed within a vacuum bag.

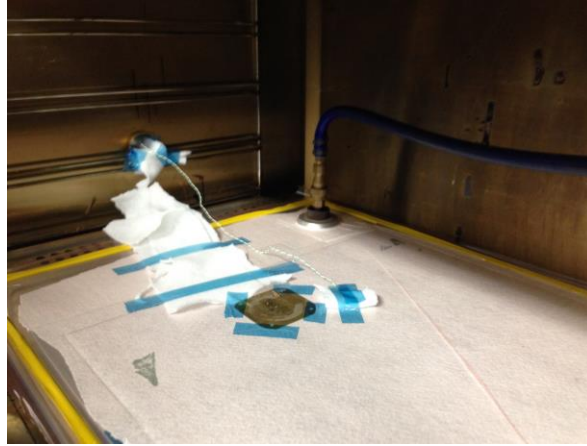


Figure 9. Coils taped to the outside of the vacuum bag.

The coils (which coupled to the embedded sensor) were placed onto the vacuum bag directly above the embedded sensor (Figure 9). The inductive coupling between coils outside of the bag, and the embedded sensor allowed for wireless ultrasonic measurements to be made, without piercing the vacuum bag (Figure 9). The composite plate was cured within an oven at a temperature of 110°C for 75 minutes. A vacuum pump was used to apply a pressure of 1 bar to the curing composite plate, for the duration of the curing cycle. Ultrasonic measurements were recorded using the ICTS throughout the cure cycle of the glass fiber epoxy plate.

3.2 Experimental method

Table 5. Effective input signal parameters.

Number of cycles	Centre frequency (KHz)	Window
5	160	Gaussian

A combined digital-oscilloscope signal-generator unit (HS3, TiePie Engineering) was used to generate an excitation signal with a peak-peak voltage equal to 24 Volts. The parameters describing the effective toneburst input are shown in Table 5. The input signal was transmitted, via the inductive coupling between the transmitting and embedded coils. The input signal transmitted to the embedded sensor, resulted in the generation of guided elastic waves (Lamb waves). Guided waves are characterized by their ability to propagate large distances, and are therefore an attractive option for long range detection. However, the waves are also dispersive with multiple wave modes existing at any given frequency. To reduce these effects, the ICTS works at a relatively low frequency-thickness product (0.53 MHz), which reduced the number of generated wave modes. The guided waves generated by the embedded piezoelectric disk transducer (16mm diameter, 0.3 mm thick transducers, manufactured from NCE51 piezoelectric material, supplied by Noliac group) were dominated by the fundamental symmetric wave mode (S_0). The attenuation of the S_0 due to material damping is significantly less than that of the fundamental flexural mode (A_0), which also exists at an operating frequency of 160KHz. The selected piezoelectric disk transducer operates in an axisymmetric radial mode, which provides increased sensitivity to the in-plane dominated motion of the S_0 mode. This system enabled the cure of the large glass fiber plate shown in Figure 8a to be monitored using a single embedded sensor in a pulse echo configuration.

The cure of the composite plate (Figure 8a) was monitored by measuring the pulse echo response throughout the cure cycle. The identification of edge reflections within the plate, allowed both the velocity, and amplitude of the received edge reflections to be recorded throughout the curing process. During the cure of a composite material, the polymer matrix undergoes significant physical changes. The changes of state, and development of mechanical properties of the curing composite were directly related to the ultrasonic parameters of the propagating acoustic waves. A user developed

program was created in commercially available software (Matlab 2013b), the program transmitted the input signal to the embedded sensor and recorded the received pulse echo response at 30 second intervals for the duration of the cure process. The program provided a live display allowing the curing composite to be monitored in real time. The cure monitoring performance of the ICTS was benchmarked against DSC. Cure analysis using DSC is well established for this process and measures the thermal response of a curing composite sample (micro scale sample)^{9,11,12}. To allow for the results of the ICTS and DSC to be directly compared, the same temperature profile was applied to the DSC sample as was applied to cure the large plate monitored by the embedded sensor.

3.3 Results

Both the amplitude of the received edge reflections, and velocity of the S_0 wave mode are plotted in Figures 10a and b respectively. The edge reflections plotted (Echoes 1 and 2, Figures 10a and b), correspond to the arrivals of the S_0 wave mode from the two closest edges to the embedded sensor (Figure 8a). Example data sets used to construct Figures 10a and b, are shown in Figures 11a,b,c and d, for various times in the cure cycle. Discussion of the implications of these results at various stages during the cure cycle is presented below.

i) Stage 1 (0-6 minutes)

The ICTS identified the reflections from the two closest edges (Figures 10a and b) prior to any cure reaction taking place. Example pulse echo data is shown in Figure 11a. Prior to curing the amplitude of the received reflections is relatively low (Figure 10a). There is a slight difference in the velocity values (Figure 10b), indicating different bulk stiffness values in each of the glass fiber plate's two principal directions.

ii) Stage 2 (7 minutes)

Upon application of an elevated temperature, the viscosity of the resin decreased. Which was accompanied by a significant increase in the attenuation experienced by the propagating acoustic waves, preventing identification of the reflections after 7 minutes into the cure cycle (Figures 10a and b). The pulse echo data during this stage of cure is shown in Figure 11b.

iii) Stage 3 (53-65 minutes)

The reflections became identifiable after 53 minutes into the cure cycle. The subsequent sharp rise in the amplitude of the received signals (Figure 10a due to a reduction in the attenuation experienced by the propagating waves, was caused by solidification of the curing epoxy resin^{7,8,9}. The velocity data plotted in Figure 10b shows a steady increase, indicating an increase in the elastic modulus of the curing resin. Figure 11c plots the pulse echo response within this region.

iv) Stage 4 (65 minutes onward)

Towards cure completion the ultrasonic data shows subtle changes in both the amplitude (Figure 10a) and velocity (S_0 wave mode, Figure 10b). Both of the data sets plateaued by 100 minutes, indicating cure completion. The velocity (Figure 10b) measurements were sensitive to changes in bulk modulus, caused by further solidification of the curing epoxy matrix. Figure 11d plots the pulse echo response. This final stage of curing represents an important region in the cure of thermoset resins, as it is responsible for controlling the glass transition temperature of the produced composite part⁹.

The results obtained from the DSC analysis (Figure 10c) are in good agreement with those of the ICTS. The large increase of measured heat flow at approximately 50 minutes is due to the exothermic curing reaction occurring in the prepreg sample, and indicates cure initiation. This coincides with the rapid increase in amplitude of received signal observed in Figure 10a. The heat flow then reduces as the rate of cure decreases. The DSC data is then seen to plateau at a similar time to the data obtained by the ICTS (at approximately 100 minutes).

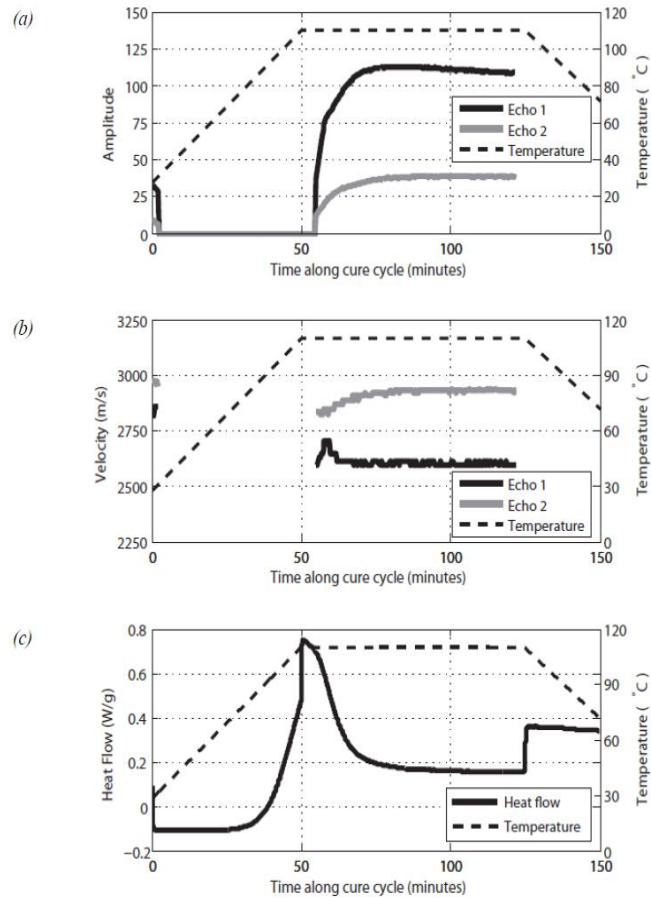


Figure 10a. Amplitude of the received edge reflections b. Velocity of the reflected S_0 waves. c. Heat flow recorded using DSC.

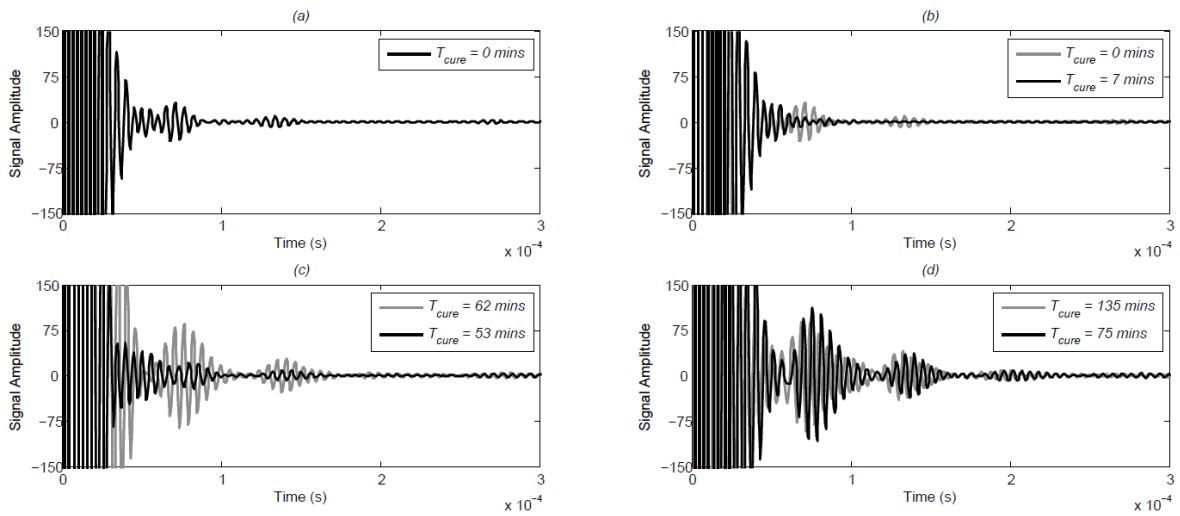


Figure 11. Guided wave pulse echo response at various times in the curing process.

4. CONCLUSION

The interlaminar shear strength testing successfully identified an encapsulating layer for the sensors that was capable of forming a strong mechanical bond, whilst providing electrical insulation to the inductance coil.

The flexural strength testing demonstrated two different embedding techniques (formed and cut ply methods, Figures 4a and b), that allow sensors to be integrated into composite structures without significantly reducing their mechanical performance, however the influence of the sensors strength was not investigated. To identify the effect of sensor strength a new series of tests will be carried out with the sensors embedded in structurally critical regions. To evaluate the impact of fiber waviness caused by embedding formed sensors, the flexural strength data set will be expanded to include a wider range of embedding locations (including structurally critical regions) for sensors embedding using the forming technique.

The cure monitoring results obtained using the ICTS are in agreement with those recorded using DSC. The techniques show a similar level of sensitivity to the curing process, indicating that the ICTS is highly sensitive to the cure of composite materials, however the micro scale sample measured using DSC, and macro scale plate monitored by the ICTS are likely to have different thermal profiles; which would influence the curing process of each sample. To enable the performance of the ICTS to be more accurately evaluated, dielectric spectroscopy (a macro scale cure monitoring technique⁹) will be used to benchmark the performance of the ICTS, allowing measurements to be made from the same sample.

REFERENCES

- [1] Diamanti, K., and C. Soutis. "Structural health monitoring techniques for aircraft composite structures." *Progress in Aerospace Sciences* 46.8 (2010): 342-352.
- [2] Zhong, C.H., Croxford A.J, Wilcox P. D., "Investigation of inductively coupled ultrasonic transducer system for NDE." *Ultrasonics, Ferroelectrics, and Frequency Control, IEEE Transactions on* 60.6 (2013): 1115-1125.
- [3] Zhong, C. H., A. J. Croxford, and P. D. Wilcox. "Remote inspection system for impact damage in large composite structure." *Proceedings of the Royal Society of London A: Mathematical, Physical and Engineering Sciences*. Vol. 471. No. 2173. The Royal Society, 2015.
- [4] Shivakumar, K, and L Emmanwori. "Mechanics of failure of composite laminates with an embedded fiber optic sensor." *Journal of composite materials* 38.8 (2004): 669-680.
- [5] White, S. R., & Hahn, H. T. (1993). Cure cycle optimization for the reduction of processing-induced residual stresses in composite materials. *Journal of Composite Materials*, 27(14), 1352-1378.
- [6] Loos, A. C., & Springer, G. S. (1983). Curing of epoxy matrix composites. *Journal of composite materials*, 17(2), 135-169
- [7] Schmachtenberg, E., Zur Heide, J. S., & Töpker, J. (2005). Application of ultrasonics for the process control of Resin Transfer Moulding (RTM). *Polymer testing*, 24(3), 330-338.
- [8] Shepard, D. D., and K. R. Smith. "A new ultrasonic measurement system for the cure monitoring of thermosetting resins and composites." *Journal of thermal analysis* 49.1 (1997): 95-100.
- [9] Challis, R. E., Unwin, M. E., Chadwick, D. L., Freemantle, R. J., Partridge, I. K., Dare, D. J., & Karkanis, P. I. (2003). Following network formation in an epoxy/amine system by ultrasound, dielectric, and nuclear magnetic resonance measurements: A comparative study. *Journal of Applied Polymer Science*, 88(7), 1665-1675.
- [10] Lin, M., & Chang, F. K. (2002). The manufacture of composite structures with a built-in network of piezoceramics. *Composites Science and Technology*, 62(7), 919-939.
- [11] Hardis, R., Jessop, J. L., Peters, F. E., & Kessler, M. R. (2013). Cure kinetics characterization and monitoring of an epoxy resin using DSC, Raman spectroscopy, and DEA. *Composites Part A: Applied Science and Manufacturing*, 49, 100-108.
- [12] Min, B. G., Hodgkin, J. H., & Stachurski, Z. H. (1993). The dependence of fracture properties on cure temperature in a DGEBA/DDS epoxy system. *Journal of applied polymer science*, 48(7), 1303-1312.